Smart Structures and Systems, *Vol. 14, No. 6 (2014) 1173-1196*
DOI: http://dx.doi.org/10.12989/sss.2014.14.6.1173

Effects of interface delay in real-time dynamic substructuring tests on a cable for cable-stayed bridge

Maria Rosaria Marsico*

College of Engineering, Mathematics and Physical Sciences, University of Exeter, North Park Road, EX4 4QF, Exeter, United Kingdom

(Received May 15, 2014, Revised August 3, 2014, Accepted August 25, 2014)

Abstract. Real-time dynamic substructuring tests have been conducted on a cable-deck system. The cable is representative of a full scale cable for a cable-stayed bridge and it interacts with a deck, numerically modelled as a single-degree-of-freedom system. The purpose of exciting the inclined cable at the bottom is to identify its nonlinear dynamics and to mark the stability boundary of the semi-trivial solution. The latter physically corresponds to the point at which the cable starts to have an out-of-plane response when both input and previous response were in-plane. The numerical and the physical parts of the system interact through a transfer system, which is an actuator, and the input signal generated by the numerical model is assumed to interact instantaneously with the system. However, only an ideal system manifests a perfect correspondence between the desired signal and the applied signal. In fact, the transfer system introduces into the desired input signal a delay, which considerably affects the feedback force that, in turn, is processed to generate a new input. The effectiveness of the control algorithm is measured by using the synchronization technique, while the online adaptive forward prediction algorithm is used to compensate for the delay error, which is present in the performed tests. The response of the cable interacting with the deck has been experimentally observed, both in the presence of delay and when delay is compensated for, and it has been compared with the analytical model. The effects of the interface delay in real-time dynamic substructuring tests conducted on the cable-deck system are extensively discussed.

Keywords: real-time dynamic substructuring; cable-deck interaction; delay compensation; time lag; adaptive forward prediction

1. Introduction

Testing is a noteworthy practice, widely used in all the branches of engineering. There are various techniques that are typically adopted to test structures, such as using shacking table (Negro *et al*. (1997)), or conducting hybrid tests (Horiuchi *et al*. (1999), Nakashima and Masaoka (1999)). In the last decades, hybrid tests started to be widespread, in particular because they combine the study of complex models with the restriction of laboratories space.

Real-time dynamic substructuring (RTDS) is a kind of hybrid testing technique. It is very powerful, especially in the presence of a nonlinear, and hence difficult to model, element within a largely linear structure (Wilson *et al*. (1973)). Essentially, the whole system is divided into two

∗Corresponding author, Lecturer, E-mail: m.r.marsico@exeter.ac.uk.

http://www.techno-press.org/?journal=sss&subpage=8 ISSN: 1738-1584 (Print), 1738-1991 (Online)

parts. One part of the system is physically built in the laboratory. The remaining part is modelled in the computer and it interfaces with the physical model - see Marsico *et al*. (2009b), Bursi and Wagg (2008), Blakeborough *et al*. (2001), and references therein for an extensive discussion.

RTDS has been used in many branches of engineering (Reinhorn *et al*. 2004, Bursi and Wagg 2008, Gawthrop *et al*. 2009, Dion *et al*. 2011, 2012), with the advantage that the parameters of the numerical model can be easily varied, without any physical change. Therefore, the behaviour of the physical model can be observed in different environments, and can validate the theory more accurately. RTDS technique has been adopted for the present research, to conduct tests on a scaled bridge's cable that interacts with the deck (Marsico *et al*. 2011b). The model has been developed by Macdonald *et al*. (2010) and, furthermore, it has been implemented by the author and validated by experimental tests (Marsico *et al*. 2011a). Experimental results have then compared with the mathematical model of the cable, which has been implemented by using the numerical continuation software AUTO (Doedel *et al*. 2000). In particular, tests have been focused on the prediction of the behaviour of the cable under unexpected loads, generated by either seismic events or wind and traffic vibrations.

A scaled model of the cable has been built at the Earthquake Engineering Research Laboratory of the University of Bristol, UK, to experimentally evaluate its behaviour. The inclined cable is fixed at the top and interacts at the bottom with a transfer system, which is a hydraulic vertical actuator. On the other hand, the deck is modelled numerically as a single-degree-of-freedom system and its parameters, such as mass, M, stiffness, K, and damping, C, can be changed in real-time (Gattulli *et al*. 2004, Srinil *et al*. 2004).

The numerical model of the deck generates the input displacement. The latter is acquired by the transfer system, which is an actuator that in turn excites the cable at the bottom by applying the corresponding force. The force is then acquired and closes the control loop by feeding back to the numerical model, and a new input displacement is generated.

The time lag between the desired input signal and the actual applied signal affects significantly the interpretation of the results, and then the reliability of capturing the behaviour of the cable. Thus, delay must be considered and accurately compensated in order that the acquired data is reliable.

Several approaches have been proposed to compensate for the transfer system error in RTDS tests. Delay compensation schemes are typically used to adjust the control loop. Typically, they include additional control algorithms as presented by Wallace *et al*. (2005b), that uses a more generic approach than the single step algorithms presented by Darby *et al*. (2001), or by Neild *et al*. (2002) via the use of model reference adaptive controller as an outer-loop control strategy. An alternative approach that uses the energy balance of the system as an overall error indicator is proposed by Ahmadizadeh and Mosqueda (2009). Wu *et al*. (2012) have recently proposed a nearly-perfect compensation method, characterized by delay over-compensation and optimal feedback.

The main issue of introducing delay compensation in RTDS tests is that the delay time of the actuators varies slightly, depending on the excitation frequency and amplitude. Moreover, each hydraulic actuator has its own response delay, therefore the frequency range for stable calculation is varied case by case (Londoño *et al*. 2012).

The author, beside several approaches already in use to compensate for delay in RTDS tests (Chen and Ricles 2008, Mercan and Ricles 2008, Ahmadizadeh *et al*. 2008), considers the online adaptive forward prediction technique. This technique removes the need for tuning both magnitude of the forward prediction and amplitude gain for each of the different excitation conditions. The adaptive forward prediction algorithm is adopted to create a new reference signal in the time domain. The reference signal is used as the transfer system demand, then eliminating the response delay and obtaining nominally zero synchronization error between each transfer system and its numerical model - see Wallace *et al*. (2005b) for an in-depth discussion on the forward prediction algorithm.

This strategy aims to achieve synchronization between the desired interface displacement of the numerical model and the effective displacements at the bottom of the physical model. An application of the online adaptive forward prediction algorithm recommended by Wallace *et al*. (2005b) is presented and the experimental RTDS tests are discussed.

This paper is concerned with the significant effects of delay compensation on the reliability of the results in RTDS tests. Section 2 is devoted to cable-deck interaction, which is analytically predicted and experimentally observed. In Section 2.1 the theoretical model that has been used to predict the behaviour of the cable-deck system is described. In Sections 2.2 and 2.3 the experimental setup, the nondimensional scaling parameters and the quantification of the damping ratio are explained.

In Section 3, a schematic diagram of the real-time substucturing loop is shown, and the process of transferring the input from the numerical model to the physical model is described. In Section 3.1, the online adaptive forward prediction algorithm is presented. In Section 3.2, the parameters of the deck and the measurement of the effectiveness of the control algorithm by synchronization subspace plots are introduced.

Section 4 is concerned with the effect of delay on the reliability of the results in RTDS tests. The online adaptive prediction forward algorithm is applied to perform the experimental tests.

Moreover, implications of delay compensation on the reliability of the results, for a wide range of excitation frequencies, are considered. The divergence between the experimental tests conducted in the absence of delay compensation and the ones conducted in the presence of delay compensation is also discussed.

2. Cable-deck interaction

2.1 Analytical model

The theory developed to define cable-deck interaction considers a single-degree-of-freedom system, as shown in Fig. 1. The mass-spring-damper model simulates the behaviour of a bridge deck, which is connected at the lower end of an inclined cable - notation *b* in Fig. 1. The angle of inclination of the cable, θ, is measured from the horizontal line in the gravity plane.

The cable is vertically excited at its lower (deck) support at a frequency close to the second natural frequency of the cable and leading the cable to experience in-plane and out-of-plane vibrations. When in-plane excitations provoke direct in-plane vibrations of the cable, the cable localised stability is identified. It occurs for natural frequencies, satisfying the relationship $\omega_{z2} = \omega_{y2} = 2\omega_{y1}$, where the subscripts *z* and *y* state for in-plane and out-of-plane respectively and the subscripts 1 and 2 state for the first and the second mode. As a consequence, the direct excitation of the second in-plane mode, ω_{z2}, affects the stability of other out-of-plane modes, ω_{y2} and $2\omega_{y1}$ (Lilien and Pinto Da Costa 1994, Marsico *et al*. 2009a).

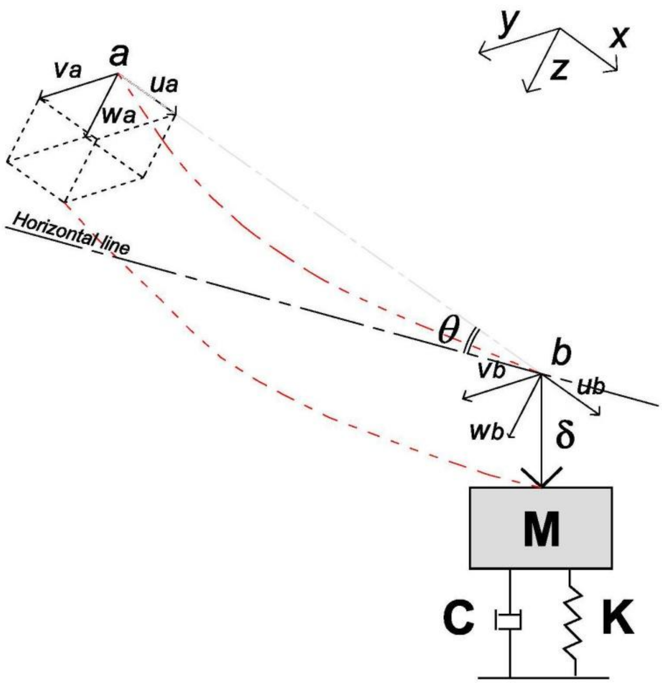

Fig. 1 Cable-deck interaction phenomena

The out-of-plane and in-plane natural frequencies, ω_{yn} and ω_{zn} respectively, are given by

$$\omega_{yn} = \frac{n\pi}{L}\sqrt{\frac{\sigma_s}{\rho}} \quad \text{and} \quad \omega_{zn} = \frac{n\pi}{L}\sqrt{\frac{\sigma_s}{\rho}\left(1+k_n\right)} \tag{1}$$

where L is the effective cable length; σ_s is the cable static stress, ρ is the density (Warnitchai *et al*. 1995). The factor k_n represents the effect of sag and it is

$$k_n = \left(\frac{2\lambda^2}{\pi^4 n^4}\right)\left(1+\left(-1\right)^{n+1}\right)^2$$

where λ^2 is Irvine's parameter (Irvine 1981).

The equation of the motion of the deck, as single-degree-of-freedom system, is

$$M\ddot{\delta} + C\dot{\delta} + K\delta + T_d \sin(\theta) = F_e \tag{2}$$

where M, C and K are respectively mass, damping and stiffness of the oscillator and δ is the deck displacement. T_d is the dynamic tension of the cable, which is obtained from the cable dynamic stress, and it also includes a static component, due to pretensioning and self-weight (Macdonald *et al*. 2010). The external excitation force is given by $F_e = F \sin(\Omega t)$, where F is the amplitude of the excitation force and Ω is the forcing frequency for the cable - for details on the vibrations of taut cables see Wagg and Neild (2010).

Finally the dynamic tension in the cable is

$$T_d = EA\varepsilon = EA\left[\frac{E_q}{E}\left(\frac{u_b - u_a}{L}\right) + \frac{\gamma}{\pi\sigma_s}\sum z_n \frac{1}{n}\left(1+(-1)^{n+1}\right) + \frac{\pi^2}{4L^2}\sum n^2\left(y_n^2 + z_n^2\right)\right] \tag{3}$$

where u, v and ω are axial, out-of-plane transverse and in-plane transverse displacements of the cable respectively - see Fig. 1. E is the Young's modulus, $E_q = \dfrac{1}{\dfrac{\lambda^2}{12}+1}E$ is the effective axial modulus, A is the cross section area, and γ is the distributed weight perpendicular to the cable cord. Subscripts a and b denote the top and bottom anchorage points respectively; subscripts d and s denote the dynamic and the static value - for details on a nonlinear dynamic model for cable see Warnitchai *et al*. (1995).

The derivation of the equations of motion of the cable-deck system has been extensively discussed in Marsico *et al*. (2009b), but for completeness will be briefly described here also.

Noting that $\omega_{y1} \neq \omega_{z1}$ due to the sag, the equalities $\omega_1 = \omega_{y1}$ and $\omega_2 = \omega_{y2} = \omega_{z2}$ can be written (as for even n, $k_n=0$). Assuming that the response of other modes is negligible in the studied frequency range $\Omega \approx 2\omega_1$, the equations of motion for the first in-plane and the first and the second out-of-plane modes can then be derived. Finally, the deck equation, along with the compatibility equation, is also written. It is worth saying that the deck natural frequency, ω_g, is affected by both deck stiffness and cable stiffness, such as

$$\omega_g = \sqrt{\frac{K + \dfrac{E_q A}{L}\sin^2(\theta)}{M}} = \sqrt{\frac{K_g}{M}} \tag{4}$$

Using the analysis proposed in Gonzalez-Buelga *et al*. (2008) but extending it to include the deck contribution, the equations are scaled by using the small parameter ε, such that they are in the standard Lagrange form. The forcing frequency, Ω, and the oscillator (i.e., global mode) frequency, ω_g, are close to twice the first out-of-plane natural frequency. Therefore $\Omega = \omega_2(1+\mu)$ and $\omega_g^2 = \omega_2^2 + \sigma$, where μ is the frequency detuning parameter, which may be expressed as $\mu = \varepsilon\hat{\mu}$ since it is small; $\sigma = 2\omega_2^2\alpha$, where $\alpha = (\omega_g / \omega_2) - 1$. Using this, taking into account that $\omega_2 = 2\omega_1$ and applying the time transform $\tau = (1+\mu)t$, the scaled equations of motions can be written. These equations are now in a form which can be averaged - see Verhulst (1996) for more details on the averaging method.

The purpose of exciting the cable at the bottom is to identify the stability boundary of the semi-trivial solution. The latter physically corresponds to the point at which the cable starts to have an out-of-plane response when both input and previous response were in-plane. Low external excitation frequencies typically lead to direct in-plane motions of both cable and oscillator. Whereas, by increasing the amplitude of the excitation force, either of the out-of-plane modes can be experienced, marking the boundary of the semi-trivial solution in the chosen parameter space.

For excitation of either out-of-plane mode, there must be a localized instability about the zero amplitude response for that mode. To find the boundary of the semi-trivial solution in the parameter space, the localized stability of each out-of-plane mode about the zero point has been examined, assuming that the other out-of-plane mode has zero averaged amplitude. For the first out-of-plane mode

$$\begin{Bmatrix} y'_{1ca} \\ y'_{1sa} \end{Bmatrix} = \varepsilon \begin{bmatrix} a\ b \\ c\ d \end{bmatrix} \begin{Bmatrix} y_{1ca} \\ y_{1sa} \end{Bmatrix} \tag{5}$$

where, following the notation in Gonzalez-Buelga *et al*. (2008)

$$\begin{aligned} a &= -\xi_{y1}\omega_1 + \frac{N_1\delta_{sa}}{4\omega_1} \\ b &= -\frac{N_1\delta_{ca}}{4\omega_1} - \mu\omega_1 + \frac{W_{12}Z_{2a}^2}{4\omega_1} \\ c &= -\frac{N_1\delta_{ca}}{4\omega_1} + \mu\omega_1 + \frac{W_{12}Z_{2a}^2}{4\omega_1} \\ d &= -\xi_{y1}\omega_1 - \frac{N_1\delta_{sa}}{4\omega_1} \end{aligned} \tag{6}$$

where ξ_{zn} and ξ_{yn} are the damping rations, Z_{2a} is the response with the contribution from only the in-plane mode, $\Delta^2 = \delta_{ca}^2 + \delta_{sa}^2$, and

$$W_{nk} = \nu_{nk}/m, \quad N_n = 2\eta_n \sin\theta / m \tag{7}$$

$$\nu_{nk} = \frac{EA\pi^4 n^2 k^2}{8L^3}, \quad \eta_n = \frac{E_q A\pi^4 n^2}{4L^2}$$

where $m=m_{yn}=m_{zn}$ is the modal mass $m=\rho AL/2$. Subscripts c and s denote the sine and cosine components of δ respectively.

It is noted that initially when the excitation amplitude is small (such that Δ and Z_{2a}^2 are small) the eigenvalues of the matrix have negative real parts and hence the stable solution set is from zero excitation up to the boundary at which the real part of one of the eigenvalues is zero. This stability boundary is given by

$$W_{12}^2 Z_{2a}^4 - 8W_{12}\mu\omega_1^2 Z_{2a}^2 + 16\omega_1^4\left(\mu^2 + \xi_{y1}^2\right) - N_1^2\Delta^2 = 0 \tag{8}$$

Using the same technique for the second out-of-plane mode and remembering that $\omega_2=2\omega_1$ and $W_{22}=4W_{12}$, the stability boundary is defined by

$$3W_{12}^2 Z_{2a}^4 - 32W_{12}\mu\omega_1^2 Z_{2a}^2 + 64\omega_1^4\left(\mu^2 + \xi_{y2}^2\right) = 0 \tag{9}$$

Note that for $\mu<3\xi_{y2}$ the second out-of-plane mode is stable about the zero amplitude position for all Z_{2a} and hence for all oscillator amplitudes Δ. Ignoring any influence of the cable on the deck except for its effective stiffness, the steady state displacement of the oscillator is:

$$\delta_{sa} = \frac{-\xi_g \omega_g \omega_2 F}{2M\left(\left(\xi_g \omega_g \omega_2\right)^2 + \left(\mu\omega_2^2 - \frac{\sigma}{2}\right)^2\right)} \tag{10}$$

$$\delta_{ca} = \frac{\left(\mu\omega_2^2 - \frac{\sigma}{2}\right)^2 F}{2M\left(\left(\xi_g \omega_g \omega_2\right)^2 + \left(\mu\omega_2^2 - \frac{\sigma}{2}\right)^2\right)}$$

and the response in the in-plane second mode is

$$16\omega_1^4 B^2 \Delta_a^2 = 64\omega_1^4\left(\mu^2 + \xi_{z2}^2\right)Z_{2a}^2 - 48\omega_1^2 \mu W_{12} Z_{2a}^4 + 9W_{12}^2 Z_{2a}^6 \tag{11}$$

In order to calculate the first out-of-plane mode stability boundary, Eqs. (8) and (11) have to be solved simultaneously.

The stability boundaries shown in Figs. 9-12 have been derived by following the aforementioned theory. In the analysis, the deck damping ratio is taken to be 1%, which is a reasonable value if compared with the damping of the cable.

2.2 Experimental set up

The cable available at the Earthquake Engineering Research Laboratory (EERL) of the University of Bristol, UK, is a single wire steel cable with diameter $0.78 \cdot 10^{-3}$ m and length 5.4 m, inclined at an angle θ=22.6°. It has been designed to reproduce the behaviour of a real cable in a cable-stayed bridge. In accordance with this purpose, 21 lead masses have been attached, spaced at 0.25 m, except the one on the top and the one on the bottom that distance 0.20 m by the ends of the cable (Gonzalez-Buelga *et al*. 2008, Marsico *et al*. 2011c). The cable interacts with the numerical model of the deck through a vertical actuator. A schematic diagram and a picture of the experimental setup are shown in Figs. 2 and 3.

The real cable stays on the Second Severn Crossing, a motorway bridge in the South West of the United Kingdom (Macdonald *et al*. 1997). This bridge has been chosen to be a specimen because it is currently monitored through a complete monitoring system, installed since its construction (1989-1996). The acquired measurements have been conveniently used to design the scaled cable to test in the laboratory.

The parameters that significantly influence the similitude of the scaled cable with the real cable have been non dimensionalised. This approach enables the definition of a general theory on a single cable interacting with the deck, which might be extended to any inclined cable with the same nondimensional parameters. The coupled effects of two or more cables have not been part of this investigation. Table 1 shows the static strain of both cables, $\varepsilon_S = T_S/EA$, where T_s is the static tension, E is the Young's modulus, A is the cross sectional area, and the ratio of both cables weight to the tensions respectively, $\Gamma = mgL/T_s$, where g is the gravitational acceleration, m is the mass per unit length and L is the effective length of the cable, including the sag.

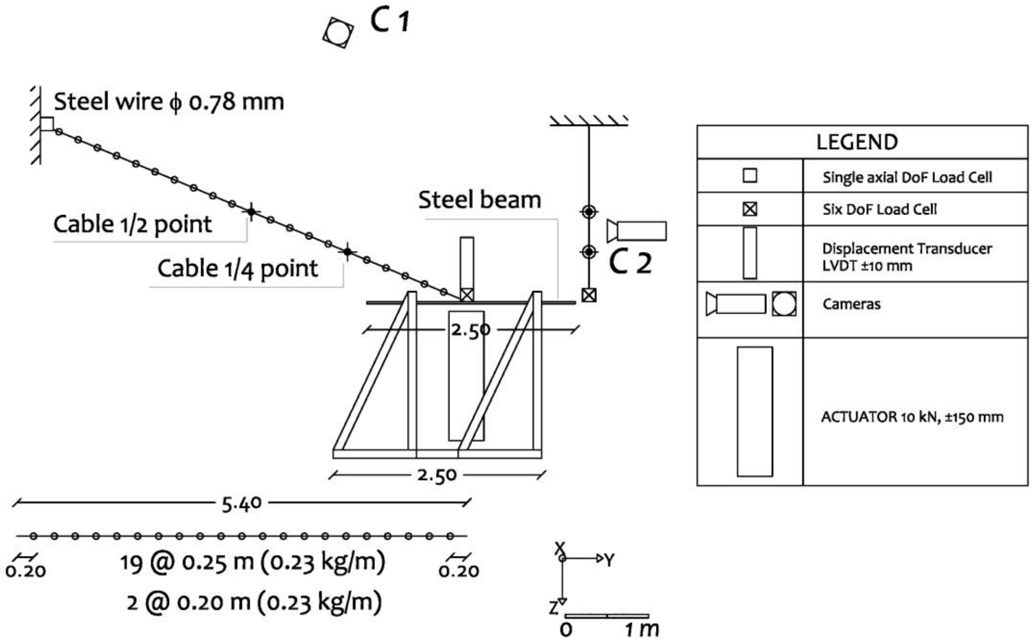

Fig. 2 Schematic diagram of the experimental setup. C_1 and C_2 state for cameras 1 and 2 respectively. Dimensions are in meters

The dynamics of a cable are mightily sensitive to the variations of the above mentioned parameters. Other relevant cable's parameters are the angle of inclination, θ, and the damping ratio ξ_n. In conformity with the parameters listed above, the Irvine's non dimensional sag parameter, which is a function of the cable geometric and elastic characteristics, and which strongly influences the symmetric modes of vibration of the cable, can then be expressed as $\lambda^2 = \Gamma^2 \cos^2 \theta / \varepsilon_s$ (Irvine and Caughey 1974).

Table 1 Non dimensional parameters

	Second Severn Crossing Cable	Model cable
$\varepsilon_s = T_s/EA$	$2.67 \cdot 10^{-3}$	$2.73 \cdot 10^{-3}$
$\Gamma = mgL/T_s$	0.0443	0.04253
$\lambda^2 = \Gamma^2 \cos^2 \theta / \varepsilon_s$	0.62	0.57
ξ_n [%]	0.10	0.02

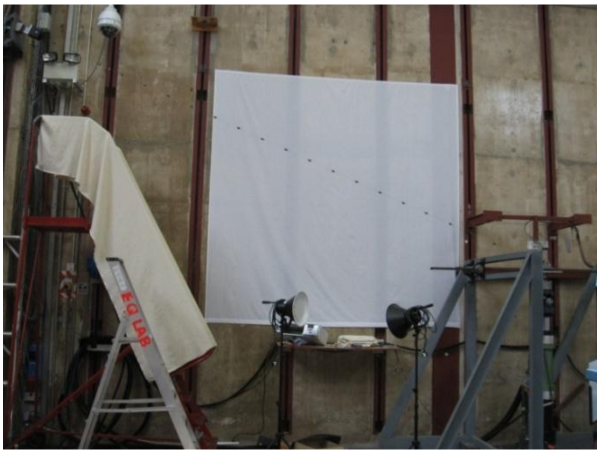

Fig. 3 Cable-deck experimental setup at Earthquake Engineering Research Laboratory, University of Bristol, UK

Table 1 also shows the damping ratio ξ_n. The difference between the damping ratio of in-situ measurements and the ones of the experimental model is essentially due to the cable sag and the internal damping, both considerably affecting the bridge's cable rather than the scaled one (Spak *et al*. 2013) - see the following Subsection 2.3 for the definition of the damping ratio.

Each test has been performed by ensuring reasonable equivalence of initial setting parameters, since they considerably vary with the external conditions. Moreover, the initial static tension, T_s, has been monitored constantly and manually adjusted to match the non dimensional parameter ε_s - see Table 1. The tension in the cable is measured by a single axial *esse* shape load cell, connected to the cable at the upper end. On the other hand, at the bottom of the cable, a multiaxial six-degree-of-freedom load cell measures the applied force, and a linear variable displacement transducer (LVDT) with limit displacement of ±10 mm, measures the vertical displacement corresponding to the applied force. The hydraulic actuator, in displacement control, is able to apply a maximum force of 10 kN and a maximum displacement of ± 150 mm.

The acquisition system consists of two cameras, one along the cable that records in-plane modes and one in front of it that records out-of-plane modes, identified respectively as C_1 and C_2 in Fig. 3.

The vibrations of 21 discretised points of the cable, which correspond to the added lead masses, are tracked by the Imetrum Video Gauge System (VGS). Although the modes of the cable are generally coupled, the dominating mode is accurately recognisable by comparing the vibrations captured by both the cameras. The VGS is ultimately used to identify the points at which parametric excitation, or modal coupling, destabilises the semi-trivial solution of either the first or the second out-of-plane mode.

2.3 Damping coefficient

The damping characteristics of a taut cable are complex and difficult to delineate. However, it is a common practice to express the damping in terms of the equivalent viscous-damping ratio, ξ_n.

This parameter shows similar decay rates under free-vibration conditions. It is defined as the natural logarithm of the ratio between two successive response amplitude peaks, Y_i and Y_{i+N} , where N>1 is the positive integer, and it is expressed as

$$\xi_n = \frac{1}{N} \ln \frac{Y_i}{Y_{i+N}} \tag{12}$$

The cable, when randomly excited, moves in-plane and out-of-plane and, as a consequence, the viscous-damping ratio, ξ_n, slightly varies according to the different free-vibration responses.

The natural frequencies of the experimental and theoretical cable are shown in Table 2 (Marsico *et al*. 2011a).

The damping ratios for the first four modes experienced by the scaled cable have been calculated via three free-vibrations tests. Table 3 shows the damping ratio for two in-plane and two out-of-plane modes, when the excitation is manually increased from Test 1 to Test 3. The interaction with the deck is not considered, therefore the deck's parameters have been neglected. For planar vibrations at low amplitude, the non-linear effects are minimised and the damping ratio is expected to be more accurate. Therefore, by averaging the values stated in Table 3, a reasonable damping ratio of ξ_n=0.02% can be assumed for the considered modes.

3. Delay compensation: method and estimation

Warnitchai *et al*. (1995) identify many possible phenomena in cable-deck interaction, especially due to the presence of nonlinear dynamics, which are difficult to model. The effects of the support motions on the cable vibration, in the form of variation of modal stiffness and the generation of forces proportional to their accelerations, are examples of such phenomena.

Moreover, the internal forces induced by the cable are, in fact, physical forces that act as concentrated forces on the structure. Those forces consist of the elastic restoring force and the inertia force, as well as of the effects of the local vibration of the cable, that generate non-linear forces and linear inertia forces. The full derivation and further considerations on those phenomena are discussed in Warnitchai *et al*. (1995).

Table 2 Cable natural frequencies [rad/sec]

	ω_{y1}	ω_{y2}	ω_{z1}	ω_{z2}
Experimental	$3.25 \cdot 2\pi$	$6.51 \cdot 2\pi$	$3.34 \cdot 2\pi$	$6.51 \cdot 2\pi$
Theoretical	$3.25 \cdot 2\pi$	$6.50 \cdot 2\pi$	$3.32 \cdot 2\pi$	$6.50 \cdot 2\pi$

Table 3 Measured damping ratio [%]

	y_2	z_2	y_1	z_1
Test 1	0.019	0.010	0.016	0.006
Test 2	0.027	0.014	0.019	0.006
Test 3	0.032	0.020	0.025	0.011

The tests conducted to identify cable-deck interaction are carried out in real-time, so that the complex dynamic behaviour is captured as accurately as possible. Furthermore, when real-time dynamic substructuring tests are conducted, the system faces dynamics that are close to the ones faced by the original structure. This enables reliable results.

In the RTDS tests conducted at EERL on a cable-deck system, the deck displacement, δ, comes from the numerical model and it is applied at the bottom of the scaled cable by a hydraulic actuator, which works as a transfer system. The excitation, in turn, passes through a horizontal steel beam that constrains the input to be strictly vertical. Then, the force required to apply a δ displacement, F_c, is measured and directly fed back to the numerical model, therefore, a new substructuring loop starts. A conceptual view of the experimental loop is shown in Figure 4.

The numerical model has been written in Matlab/Simulink and has been implemented on a dSpace DS1104 RD Controller board. Then the dSpace module ControlDesk has been used for the online analysis and control.

The cable has been previously tested without substructuring. Hence, the effective displacements acquired by the LVDT set at the bottom of the cable have been compared with the displacements of the attached middle and quarter tracks, recorded by the VGS - see Marsico *et al*. (2010) for the experimental results.

Whereas, when RTDS tests are performed, the transfer system introduces into the desirable displacement signal a delay, τ , which will significantly affect the feedback force. Generally, the input signal is assumed to interact instantaneously with the system. However, only an ideal system manifests a perfect correspondence between the desirable signal and the applied signal.

Delay is an inherent physical consequence of hybrid tests. Moreover, the systems used in the laboratories are rather complex and highly divert from the perfect synchronization. Delay error leads to a reduction in the degree of synchronization of the transfer system and thus a corresponding reduction in the accuracy of the numerical model compared to that of the emulated system (Mosqueda *et al*. 2007).

Delay in hybrid tests can be represented by two components. One, e_1, is a function that describes the accuracy of the numerical models compared to the appropriate variable in the complete emulated system. The other, e_2, represents the degree of synchronization between each transfer system and its numerical model. Both terms, e_1 and e_2, are coupled and, when substructuring complex systems, the only measure of accuracy is the degree of synchronization, e_2 - see Wallace *et al*. (2005b) for the derivations.

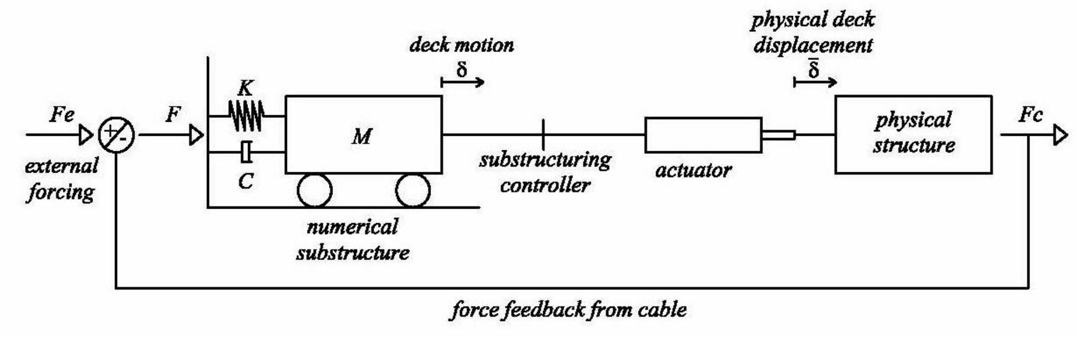

Fig. 4 Schematic description of the substructuring experimental loop

However, in practice, the synchronization error, e_2, can never be exactly equal to zero in RTDS tests. Furthermore, it affects significantly the stability of the substructuring algorithm then resulting in a corresponding error e_1. Then, a small delay, e_2, in the transfer system response introduces a corresponding error in the feedback force vector, which can be thought of as adding negative damping to the system. If the negative damping is larger, then the experiment becomes impossible (Horiuchi *et al*. 1999). The aforementioned considerations clearly prognosticate the consequences of performing substructuring tests in the presence of delay.

The effectiveness of the control algorithm is measured by using the subspace plots approach - extensively discussed in Ashwin (1998). The design interface displacement of the numerical model is plotted versus the actual position of the transfer system. Thus, the amount of delay is online predicted and a new reference signal is generated to ideally eliminate the response error.

The desired oscillator displacement coming from the numerical model is compared with the corresponding effective displacement acquired by a linear variable displacement transducer during the tests. Ideal delay compensation corresponds to narrow the ellipse that plots the desirable input displacement versus the acquired input displacement, to the maximum axis inclined at 45° and the minimum axis close to zero. Any introduced delay in substructuring tests transforms the ideal straight line into an ellipse. When the delay is greater, the width of the minor axis of the ellipse is larger.

Therefore, if δ is the target displacement coming from the substructuring model, the effective displacement takes the form

$$\overline{\delta} = \delta(t-\tau) \tag{13}$$

The effects of the undesirable dynamics introduced by the actuator into the system have been initially minimised by using an online adaptive forward prediction technique.

3.1 Online adaptive forward prediction

Wu *et al*. (2012) present an overview of the compensation schemes that have been adopted for transfer systems to reduce the negative effect of time delay. Online procedures of delay estimation and adaptive mechanisms have been used to correct the delay parameter and to account for system dynamics which in fact may be varying during the test. Those procedures include the online adaptive forward prediction (AFP) technique that is used in the RTDS tests conducted on the cable-deck system.

The adaptive forward prediction algorithm removes the need for tuning both the magnitude of the forward prediction and the amplitude gain for each different excitation condition. This tuning is a need for the basic forward prediction algorithm. Moreover, AFP algorithm achieves high levels of synchronization for frequency dependent and transient plant conditions by closing the control loop and using the feedback dynamics of the transfer system (Wallace *et al*. 2005a). This technique can appropriately be used when there is no knowledge of the plant dynamics and when there is transient or frequency dependent plant behaviour. Furthermore, it achieves a stable substructuring algorithm (Kyrychko *et al*. 2006).

The approach used here follows the adaptive forward prediction technique, which is based on a polynomial estimation algorithm to compensate for the delay present in the transfer system. The prediction algorithm is $\delta(t)' = \left(P_{N,n,\Delta}[\delta]\right)(t+\rho)$, where $\left(P_{N,n,\Delta}[\delta]\right)$ is the least squares fitting *N*th-order polynomial through the *n* time-point pairs

$(t,\delta(t)),(t-\Delta,\delta(t-\Delta)),....,(t-(n-1)\Delta,\delta(t-(n-1)\Delta))$; ρ is the amount of the forward prediction. The sampling time step, Δ, used in the RTDS tests is 1 ms for experimentation. The polynomial based forward prediction algorithm is extensively discussed in Wallace *et al*. (2005a).

The general equation of motion can be expressed as

$$M\ddot{\delta}+C\dot{\delta}+K\delta+K'\left(\bar{\delta},\dot{\bar{\delta}},\ddot{\bar{\delta}}\right)=F_e \tag{14}$$

where *K'* is the restoring force associated with the experimental substructure, which is a function of the displacement, velocity and acceleration achieved by the specimen, as well as being affected by the delay error (Wu *et al*. 2007).

3.2 Estimation of delay in RTDS tests

The prediction of the amount of delay introduced in the cable-deck system while performing RTDS tests is discussed hereinafter. The RTDS tests have been conducted by selecting the properties of the deck, such as mass, stiffness and damping, and by increasing the force that excites the second in-plane mode, to the value that drives the cable to vibrate in the not excited modes. The effect of delay error on the predictability of the behaviour of the entire cable-deck system has been observed in a selected parameter space and the ratio, *q*, between the natural frequency of the deck and the second natural frequency of the cable, expressed by ω_g/ω_2, has been fixed.

A number of RTDS tests has been conducted on the cable, when q_1=0.98, such as M_1=248 kg, K_1=10091.76 N/m and C_1=31.64 kg/s, and q_3=1.04, such as M_3=248 kg, K_3=111365.32 N/m and C_3=33.58 kg/s. These values have been selected to explore different responses of the cable, when the parameter *q* is both more and less than one (q_2=1), and then the interaction with the deck is noticeable. An extensive discussion on the experimental results for q_2=1 can be found in Macdonald *et al*. (2010).

For the purpose of the present research, both values of *q*, namely q_1=0.98 and q_3=1.04, have been adopted. However, because of the same effect of the delay error present in the system, only results for $q=q_1$=0.98 will be shown. This assumption is valid in the range of the frequencies of interest of the present research; specifically the cable has been observed in the range of the excitation frequencies of $-0.03\leq \mu \leq+0.03$, where $\mu=\Omega/\omega_2-1$ is a parameter accounting for the oscillator frequency and the second in-plane frequency of the cable.

The effectiveness of the control algorithm is measured by synchronization subspace plots. Those plots are adopted to measure the effectiveness of the control algorithm in the experimental tests conducted on the cable-deck system at EERL. A combination of exciting frequency and force, leading the cable to be stable, has been considered.

Fig. 5 shows subspace plots for tests conducted for a fix value of the parameter *q*=0.98, and with the exciting frequency and force of *f*=6.6381 Hz and *F*=125 N respectively, such as when the cable is excited and it responds in the second in-plane mode, Z_2.

In the chart on the left, the oscillator displacement coming from the numerical model (*x* axis) against the delayed oscillator displacement, which is acquired at the bottom of the cable (*y* axis), is plotted. Delay has been evaluated by essentially measuring the shift time between two sine wave excitations in the time domain and the value of τ=12 ms has been assessed - see the chart on the right in Fig. 5.

Tests have been performed by increasing delay compensation from 0 ms to 12 ms and the ellipse shape responses have been monitored. The largest external ellipse represents the system performing in the presence of a delay, while the central one, approaching to a straight line, is close to the response of an ideal system, with a compensated delay of τ=12 ms.

Furthermore, the synchronization subspace plots have been used to estimate the time lag affecting the RTDS tests when the cable faces out-of-plane modes, even though it is excited in the second in-plane mode. The cable is in fact defined as unstable.

Fig. 6 states the response of the cable shacked by sine waves exciting its second in-plane mode and marking the Z_2 stability boundary of the cable-deck system, for μ=+0.01. The chart on the top shows a test performed in absence of delay compensation. It clearly shows that the response of the system is substantially away from the ideal response, which is recognisable when the ellipse condenses in a line (Fig. 6 at the bottom).

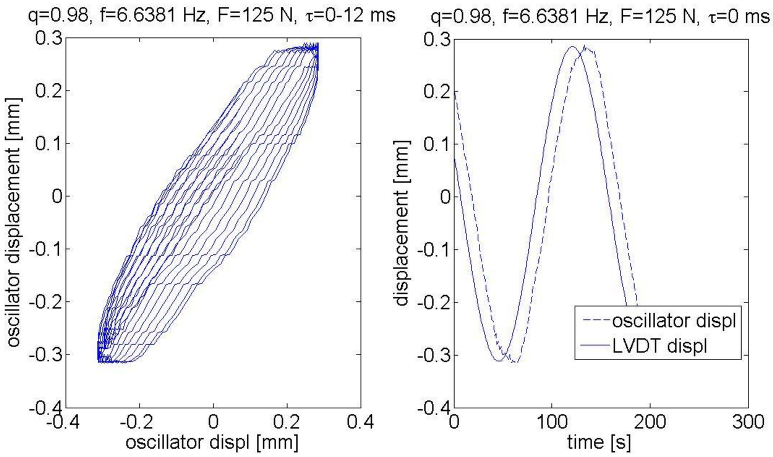

Fig. 5 Estimation of delay compensation

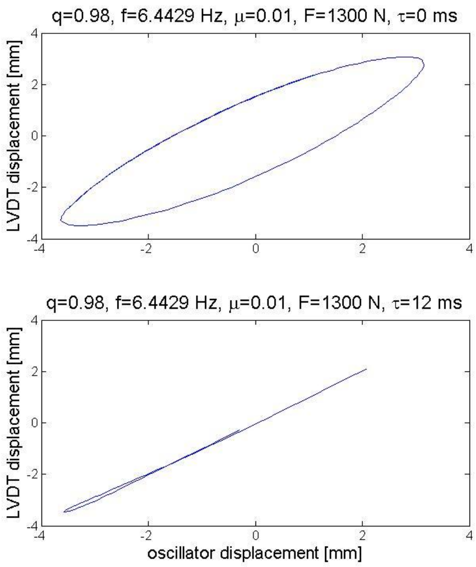

Fig. 6 Acquired vertical displacement with and without delay compensation

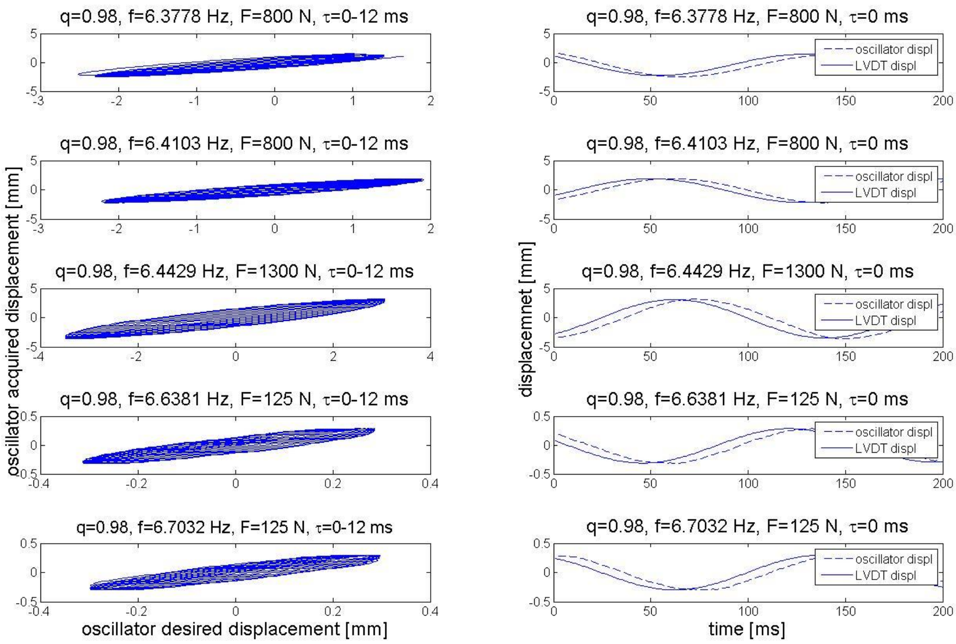

Fig. 7 Delay compensation when the excitation provokes the cables instability

A similar approach has been used when both exciting force, F, and exciting frequency, f , are varied to provoke either of the instabilities of the cable. Fig. 7 shows a consistent delay assessment for five combinations of exciting force and frequency, for μ=0.03 (Marsico *et al*. 2013a, b). Delay compensation has been increased from 0 ms to 12 ms, and the external ellipses (τ =0 ms) and the straight diagonal lines (τ =12 ms) have been drawn - see panels on the left in Fig. 7. Those results refer to the tests looking at the semi-trivial solution, which has been analytically predicted following the theory synthesized in Section 2.1. By slightly increasing the exciting input, either of force or frequency, the cable overshoots the stability boundary and chaotically responds.

The AFP algorithm has been used to compensate for the delay error present in the transfer system. The polynomial fitting parameters of N=4 and n=20, and a constant delay compensation of ρ=12 ms have been considered.

The investigation on the prediction of delay in RTDS tests performed on the cable-deck system has been restricted to a range of exciting input that gives results reliable and comparable with the analytical stability boundary curves, as shown in Figs. 9-12. For that range of exiting frequencies, the response of the cable is slightly affected by the nonlinear dynamics, which are complex to predict, and the contribution of higher modes is not significant; moreover the delay error is comparable. The response of the system for exciting frequencies outside that range has not been considered in the present research: therefore, a constant delay is a reasonable assumption.

The synchronization subspace plots in Fig. 8 show results for the performed test, in the presence of delay and with delay compensation of 12 ms. The convergence to an ideal straight line, looking at the perfect synchronization between the transfer system and the numerical model, is appreciable in the panels on the right (Marsico *et al*. 2013a,b).

Further experimental tests with delay compensation of 12 ms, for q=0.98 and μ=0.02, have been conducted to capture Z_1, Y_1, Y_2 analytical stability boundary curves and the branching bifurcation points. Those tests are extensively discussed in Marsico *et al*. (2011a).

It should be noted that further experiments ending in chaotic responses of the cable have been neglected because of the complexity of extracting the contribution of the modes. Moreover, for the present research, only the first four modes have been considered. This restriction enables comparison with the analytical model.

4. Effect of delay on RTDS tests conducted on a cable-deck system

Steady state RTDS tests have been performed on the cable-deck system to mark the stability boundaries. Fig. 9 shows the Z_2 stability boundary of the cable interacting with a deck, for q=0.98. The cable has been excited in the second in-plane mode and the maximum displacement of the quarter point has been recorded by the VGS, before that the cable vibrates in either of the out-of-plane modes. The analytical curve shown in Fig. 9, plots the normalised amplitude of the quarter point, Z_2, against the normalised applied displacement, Δ. It has been defined by following the theory on the nonlinear dynamics of the cable developed by Warnitchai *et al*. (1995) and later extended by Macdonald *et al*. (2010), and synthesised in Section 2.1. The parameter μ=+0.03 has been chosen because the S-shape is more distinguishable and the comparison with the experimental results can be appreciated.

The experimental results from tests conducted with delay compensation of 12 ms, marked with stars in Fig. 9, follow the lower boundary of the S-shape curve and also capture the second branch of the Z_2 response. The experimental points above the third upper branch of the S-shape curve predict the presence of upper Z_2 stability branches that have been analytically defined in Marsico *et al*. (2011a) for q=0.98. Whereas, the experimental results from tests conducted in the presence of delay, do not catch the three branches of the Z_2 response of the cable interacting with the deck - see the circles in Fig. 9. The circles diverge from the analytical S-shape curve, and the presence of delay, in the form as discussed in Section 3, has a significant effect on those results. Moreover, none of the two upper branches of the Z_2 response in the range of $2 \cdot 10^{-4} \leq \Delta / L \leq 3 \cdot 10^{-4}$ is captured.

Results from tests conducted on the cable-deck system slightly under-compensated show that neither the second nor the third stability boundary branch of the S-shape curve in Fig. 9 is captured experimentally.

Those tests have prudently been neglected in this paper because they do not mark any of the actual cable stability boundaries, which have been predicted analytically.

Figs. 10 and 11 show the analytical curves representing the loss of local stability of the semi-trivial solution, which is when the response is limited to the second in-plane mode. The turning point is in practice the Z_2 stability boundary in the μ domain and it corresponds to the upper branch of the S-shape Z_2 stability boundary, shown in Fig. 9 for μ=0.03. The curves are marked in the space of the normalised exciting force, F , versus μ, for both q=0.98 and q=1.04. In the area above the curves, for $\mu \leq 0$, the cable dynamics include the first out-of-plane mode component. When increasing the values of μ, other modes are triggered. The sensitive frequencies move from the left (in Fig. 10) to the right of μ = 0 (in Fig. 11) because of the deck resonant frequency contained in the parameter q. For $\mu > 0$ the cable faces the first in-plane mode before responding in the first out-of-plane mode.

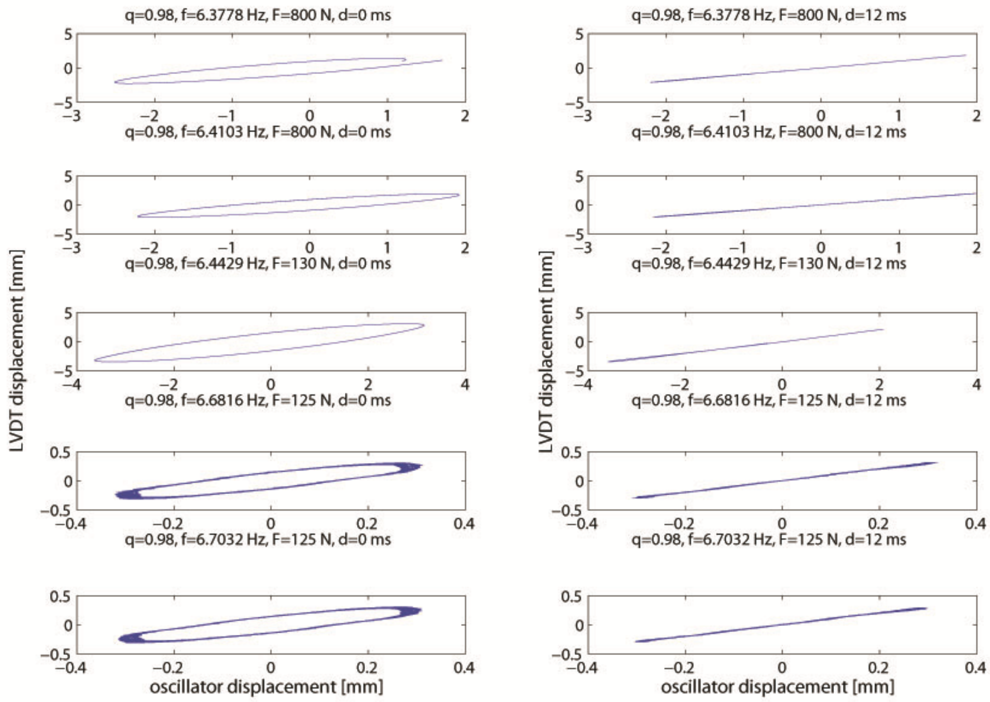

Fig. 8 Delay prediction for a range of frequencies; d states for delay

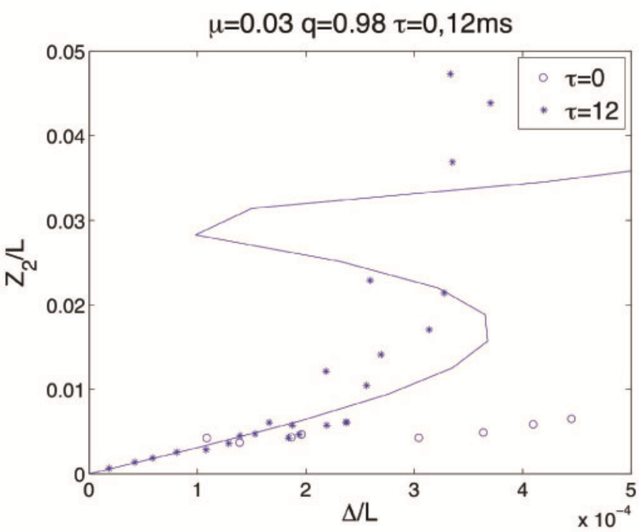

Fig. 9 Second in-plane stability boundary affected by delay compensation

In Fig. 11, a double tongue has been discovered experimentally, one tongue due to out-of-plane modes (centred around μ=0), and the other due to the first in-plane mode (centred around μ=0.025).

It should be noted that the experimental data capture the complex dynamics of the cable, which cannot be predicted analytically. The S and V shape curves have been derived by following the theory described in Section 2.1 (Warnitchai *et al*. (1995)). This theory does not include the dynamic effect of the cable on the deck, which is included in the performed RTDS tests.

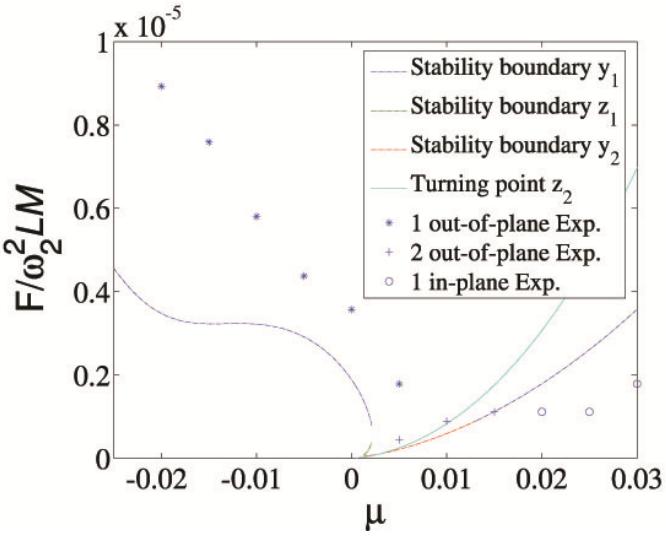

Fig. 10 Stability boundaries for q=0.98

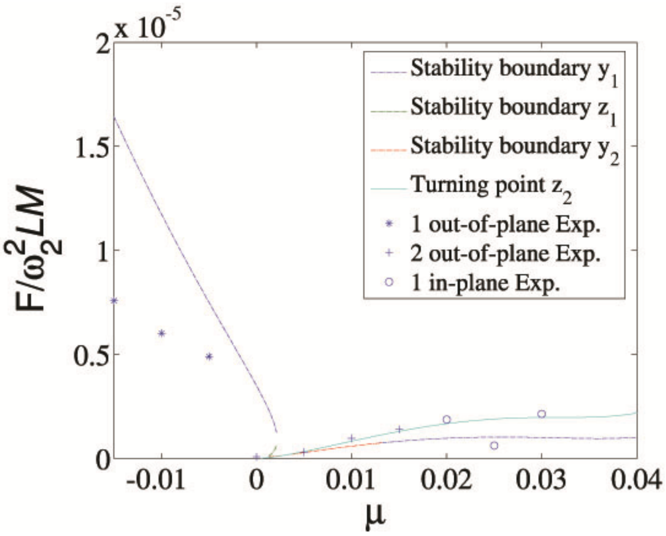

Fig. 11 Stability boundaries for q=1.04

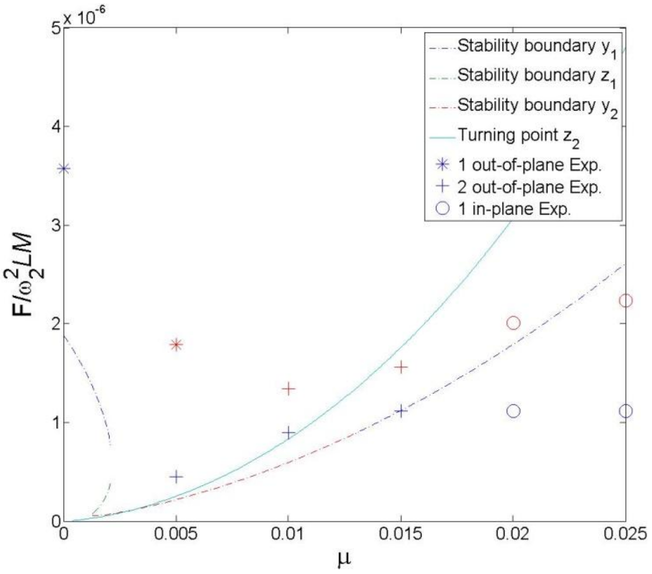

Fig. 12 Stability boundary for μ>0 and q=0.98, with delay compensation of 12 ms (blue points) and 17 ms (red points)

Although the experimental tests conducted with compensated delay of τ =12 ms capture significant aspects of the behaviour of the cable-deck system, a discrepancy between the analytical model and the experimental data is still evident in both Figs. 10 and 11. Therefore, further studies have been conducted to implement the analytical model. The continuation software AUTO (Doedel *et al*. 2000) has been used to capture further stability boundaries and bifurcation points that have been experimentally detected, and to extract the contribution of each mode. Results for q=0.98 are presented in Marsico *et al*. (2011a).

Further attempt has been made through introducing delay overcompensation. A zoom of the stability boundary curves for q=0.98, in the positive range of μ, is presented in Fig. 12. The blue points show the results for the tests conducted with a delay compensation of τ =12 ms; the red points, all above the blue ones, show the results for the tests conducted with overcompensated delay τ =17 ms. It is evident that by increasing delay compensation from 12 ms to 17 ms the lower second out-of-plane stability boundary, y_2, is not captured - see the dashed red line. For μ=0.005 a misleading first out-of-plane stability boundary is identified - red star - while the actual second out-of-plane stability boundary is exceeded. For $\mu\geq$0.01 the experimental points with τ=17 ms identify the second out-of-plane and the first in-plane stability boundaries that are comparable with those identified by the experimental points with τ=12 ms. However, input forces higher than those estimated for τ =12 ms are required. Therefore, for τ=17 ms higher stabilities branches, which are predictable analytically and which are shown in Fig. 9, cannot be localized experimentally. In fact, they would require even higher input forces that in turn would excite complex modes, by exceeding the actual stability boundaries.

Tests on the cable-deck system demonstrate that adequate delay compensation, in the range of the considered frequencies, fluctuates between 11.8 ms and 12.2 ms. However, the interpretation of the cable response is slightly affected by ±0.05%. Therefore, a convenient value of τ =12 ms has been introduced to homogenise the tests in the range of -0.03≤μ≤+0.03, without the consistency of the results being significantly jeopardised. It is worth saying that the assumption of a constant delay may not be valid either when the tests are performed outside that range, or when the cable interacts with decks that are different to those three discussed in this paper. Thus, the adoption of the online AFP technique as a delay compensation method is prudently recommended.

Horiuchi *et al*. (1999) early observed that delay compensation is sensitive to the magnitude of the exciting force. RTDS tests on the cable-deck system show that a delay compensation of 12 ms is consistent for $\chi \geq 1$, where the introduced parameter, χ, is the magnitude of the restoring force relative to the static tension in the cable, T_s=286N . The corresponding vertical displacement at the bottom edge of the cable is physically appreciable, and varies between ±1.5 mm and ±4.0 mm. Whereas, when χ<1, the vertical displacements at the bottom of the cable are inconsistent, and the time lag slightly increases up to 12.2 ms. It is worth saying that the fluctuation of delay compensation is likely due to internal errors affecting the substructuring loop, which are regardless exhibited in an accurate characterization of the system. Furthermore, the magnitude of the restoring force relative to the static tension in the cable influences the delay. This is likely due to the fact that the actuator is a nonlinear system and cannot be completely characterized by a time delay. However, in the considered range of exciting force and frequency, the actuator dynamics are consistent, therefore a constant delay compensation of 12 ms is a reasonable assumption.

Unfortunately, due to the conceptual idea of substructuring tests, where physical elements and mechanical movements interact instantaneously, time lag cannot be obviated, but it can be compensated with satisfactory accuracy. Fig. 9 shows that results from RTDS tests, conducted with a delay compensation of τ =12 ms, reasonably describe the response of the cable in the range of the considered exciting frequencies.

It is worth saying that the inception of each test is very sensitive to the amount of delay introduced into the system. The amount of the initial time lag depends on physical issues, such as the time for the oil pressure to activate the actuator and for the actuator to achieve the desirable value of the exciting force. To avoid inaccurate results, then the initial seconds of the tests have been prudently neglected.

5. Conclusions

Real-time dynamic substructuring tests have been conducted on a cable-deck system to identify the nonlinear dynamics of the cable interacting with the deck and to mark the stability boundary of the semi-trivial solution. The latter physically corresponds to the point at which the cable starts to have an out-of-plane response, when both input and previous response were in-plane. The significant effect of the interface delay in RTDS tests on the reliability of the results is extensively discussed.

The cable is physically present at the Earthquake Engineering Research Laboratory of the University of Bristol, UK, and the deck is modelled numerically as a single-degree-of-freedom system. The characteristics of the numerical model can be changed in real-time without any physical change then cable-deck interaction is thoroughly investigated. Moreover, the cable-deck system faces dynamics that are close to those faced by the original structure. Thus, many possible phenomena, especially due to nonlinear dynamics of the cable that are difficult to model, are captured.

The displacement that excites the deck comes from the numerical model.

Then, the corresponding force is applied at the bottom of the inclined cable by a hydraulic actuator, which works as a transfer system. The effects of the undesirable dynamics introduced by the actuator into the system have been minimised by using the online adaptive forward prediction technique. The latter is based on a polynomial estimation algorithm that removes the need for tuning both magnitude of the forward prediction and amplitude gain for each different excitation conditions.

The effectiveness of the control algorithm is measured by synchronization subspace plots namely the design interface displacement of the numerical model is plotted versus the actual position of the transfer system. Thus, the amount of delay is online predicted and a new reference signal is generated to ideally eliminate the response error.

It has been observed that delay compensation is sensitive to the magnitude of the exciting force and, moreover, to the excitation frequency. The fluctuation of delay compensation is likely due to internal errors affecting the substructuring loop, that regardless are exhibited in an accurate characterization of the system. Furthermore, it is likely due to the fact that the actuator is a nonlinear system and cannot be completely characterized by a time delay. In the considered range of exciting force and frequency, the actuator dynamics are consistent therefore a constant delay compensation of 12 ms has been assumed.

The experimental tests conducted with compensated delay of τ =12 ms capture significant aspects of the behaviour of the cable-deck system. However, a discrepancy between the analytical model and the experimental data is still evident. The analytical model in fact does not include the dynamic effect of the cable on the deck, which is included in the performed RTDS tests.

In addition, it has been observed that the inception of each test is very sensitive to the amount of delay introduced into the system. Therefore, the initial seconds of the tests have to be prudently neglected.

Acknowledgments

The author would like to acknowledge the support from the Engineering and Physical Sciences Research Council (EPSRC), under the grant EP/F030711/1. The author gratefully thanks Prof. D.J. Wagg for his guidance in conducting the present research, Dr. S.A. Neild and Dr. J.H.G. Macdonald for their advice on the analytical model and on the interpretation of the experimental results.

References

Ahmadizadeh, M. and Mosqueda, G. (2009), "Online energy-based error indicator for assessment of numerical and experimental errors in hybrid simulation", *Eng. Struct.*, **31**(1), 1987-1996.

Ahmadizadeh, M., Mosqueda, G. and Reinhorn, A. (2008), "Compensation of actuator delay and dynamics for real-time hybrid structural simulation", *Earthq. Eng. Struct. D.*, **37**(1), 21-42.

Ashwin, P. (1998), "Non-linear dynamics, loss of synchronization and symmetry breaking". *Proc. Inst. Mech. Eng. G.*, **212**, 183-187.

Blakeborough, A., Sieber, J., Neild, S., Wagg, D. and Krauskopf, B. (2001), "The development of real-time substructure testing", *Philos. T. R. Soc. Lond. A.*, **34**(15), 1869-1891.

Bursi, O. and Wagg, D. (2008), *Modern testing techniques for Substructural System*, Springer-Verlag.

Chen, C. and Ricles, J. (2008), "Stability analysis of sd of real-time hybrid testing systems with explicit integration algorithms and actuator delay", *Earthq. Eng. Struct. D.*, 37(4).

Darby, A., Blakeborough, A. and Williams, M. (2001), "Improved control algorithm for real-time substructure testing", *Earthq. Eng. Struct. D.*, **30**(3), 431-448.
Dion, C., Bouaanani, N., Tremblaya, R. and Lamarche, C. (2012), "Real-time dynamic substructuring testing of a bridge equipped with friction-based seismic isolators", *J. Bridge Eng.*, **17**(1), 4-14.
Dion, C., Bouaanani, N., Tremblaya, R., Lamarche, C. and Leclerc, M. (2011), "Real-time dynamic substructuring testing of viscous seismic protective devices for bridge structures", *Eng. Struct.*, **33**(12), 3351-3363.
Doedel, E., Champneys, A., Fairgrieve, T., Kuznetsov, Y., Sandstede, B. and Wang, X. (2000), *AUTO2000 and AUTO-07P: Continuation and bifurcation software for ordinary differential equations*, Department of Computer Science, Concordia University, Montreal, Canada.
Gattulli, V., Martinelli, L., Perotti, F. and Vestroni, F. (2004), "Non-linear oscillations of cables under harmonic loading using analytical and finite element models", *Comput. Method. Appl. M.*, **193**(1-2), 69-85.
Gawthrop, P., Neild, S., Gonzalez Buelga, A. and Wagg, D. (2009), "Causality in real-time dynamic substructure testing", *Mechatronics*, **19**(7), 1105-1115.
Gonzalez-Buelga, A., Neild, S., Wagg, D. and Macdonald, J. (2008), "Modal stability inclined cables subjected to vertical support excitation", *J. Sound Vib.*, **318**(3), 565-579.
Horiuchi, T., Inoue, M., Konno, T. and Namita, Y. (1999), "Real-time hybrid experimental system with actuator delay compensation and its application to a piping system with energy absorber", *Earthq. Eng. Struct. D.*, **28**, 1121- 1141.
Irvine, H. (1981), *Cable structures*, MIT Press, Cambridge, MA.
Irvine, H. and Caughey, T. (1974), "The linear theory of free vibrations of a suspended cable", *P. Roy. Soc. Lond. A.*, **341**(1626), 299-315.
Kyrychko, Y., Blyuss, K., Gonzalez-Buelga, A., Hogan, S. and Wagg, D. (2006). "Real-time dynamic substructuring in a coupled oscillator-pendulum system", *P. Roy. Soc. Lond. A.*, **462**(2068), 1271-1294.
Lilien, J. and Pinto Da Costa, A. (1994), "Vibration amplitudes caused by para-metric excitation of cable stayed structures", *J. Sound Vib.*, **174**, 69-90.
Londoño, J., Serino, G. and di Bernardo, M. (2012), "Existence and stability of limit cycles in a delayed dry-friction oscillator", *Nonlinear Dynam.*, **67**(1), 483-496.
Macdonald, J., Dagless, E., Thomas, B. and Taylor, C. (1997), "Dynamic measurements of the second severn crossing", *Proc. Instn Civ. Engrs, Transp.*, **123**(4), 241-248.
Macdonald, J., Dietz, M., Neild, S., Gonzalez-Buelga, A., Crewe, A. and Wagg, D. (2010), "Generalized modal stability of inclined cables subjected to support excitations", *J. Sound Vib.*, **329**(21), 4515-4533.
Marsico, M., Wagg, D. and Neild, S. (2010), "The effect of deck parameters on out-of-plane vibrations of a stay-bridge cable", *Proceedings of the International Conference on Noise and Vibration Engineering*, Leuven, Belgium.
Marsico, M.R., Neild, S., Gonzalez-Buelga, A. and Wagg, D. (2009a), "Interaction between in-plane and out- of-plane cable mode for a cable-deck system", Proceedings of the ASME Design Engineering technical Conference and Computers and Information in Engineering Conference, DETC.
Marsico, M.R., Sieber, J., Neild, S. and Wagg, D. (2009b), "Dynamic testing for uncertainty in structural dynamics", *Proceedings of the 2nd International Conference on Uncertainty in Structural Dynamics*, The University of Sheffield.
Marsico, M.R., Tzanov, V., Wagg, D., Neild, S. and Krauskopf, B. (2011a), "Bifurcation analysis of parametrically excited inclined cable close to two-to-one internal resonance", *J. Sound Vib.*, **24**(330), 6023-6035.
Marsico, M.R., Wagg, D. and Neild, S. (2011b), "The effect of interface dalay in substructuring experiments", *Proceedings of the ASME Design Engineering technical Conference and Computers and Information in Engineering Conference*.
Marsico, M.R., Wagg, D. and Neild, S. (2013a), *Real time dynamic substructuring tests on a cable-deck system in absence of delay*, Network for Earthquake Engineering Simulation (distributor), Dataset

DOI:10.4231/D3VX0635F.

Marsico, M.R., Wagg, D. and Neild, S. (2013b), *Real time dynamic substructuring tests on a cable-deck system in presence of delay*, Network for Earthquake Engineering Simulation (distributor), Dataset DOI:10.4231/D30P0WR0N

Marsico, M.R., Wagg, D., Neild, S. and Macdonald, J. (2011c), "Nonlinear cable vibrations: experimental tests on an inclined cable", *Proc. Eurodyn. Leuven Belgium*, 1446-1450.

Mercan, O. and Ricles, J. (2008), "Stability analysis for real-time pseudodynamic and hybrid pseudodynamic testing with multiple sources of delay", *Earthq. Eng. Struct. D.*, **37**(10), 1269-1293.

Mosqueda, G., Stojadinovic, B. and Mahin, S. (2007), "Real-time error monitoring for hybrid simulation. ii: Structural response modification due to errors", *J. Struct. Eng. - ASCE*, **133**(8), 1109-1119.

Nakashima, M. and Masaoka, N. (1999), "Real-time on-line test for mdof systems", *Earthq. Eng. Struct. D.*, **28**(4), 393-420.

Negro, P., Pegon, P. and Verzeletti, G. (1997), "Pseudodynamic capabilities of the elsa laboratory for earthquake testing of large structures", *Earthq. Eng. Struct. D.*, **12**(10), 163-180.

Neild, S., Drury, D., Wagg, D., Stoten, D. and Crew, A. (2002), "Implementing real time adaptive control methods for substructuring of large structure", *Proceedings of the 3rd World Conf. on Structural Control*, Como, Italy.

Reinhorn, A., Sivaselvan, M., Liang, Z., Shao, X., Pitman, M. and Weinreber, S. (2004), "Large scale real time dynamic hybrid testing technique - shake tables substructure testing", *Adv. Exp. Struct. Eng.*, 457-464.

Spak, K., Agnes, G. and Inman, D. (2013), "Cable modeling and internal damping developments", *Appl. Mech. Rev.*, **65**(1), 1-18.

Srinil, N., Rega, G. and Chucheepsakul, S. (2004), "Three-dimensional non-linear coupling and dynamic tension in the large-amplitude free vibrations of arbitrarily sagged cables", *J. Sound Vib.*, **269**(3-5), 823-852.

Verhulst, F. (1996), *Nonlinear differential equations and dynamical systems*, Springer.

Wagg, D. and Neild, S. (2010), *Nonlinear Vibration with Control*, Springer.

Wallace, M., Sieber, J., Neild, S., Wagg, D. and Krauskopf, B. (2005a), "Stability analysis of real-time dynamic substructuring using delay differential equation models", *Earthq. Eng. Struct. D.*, **34**(15), 1817-1832.

Wallace, M., Wagg, D. and Neild, S. (2005b), "An adaptive polynomial based forward prediction algorithm for multi-actuator real-time dynamic substructuring", *P. Roy. Soc.*, **461**(2064), 3807–3826.

Warnitchai, Y., Fujino, T. and Susumpov, A. (1995), "A nonlinear dynamic model for cables and its application to a cable structure-system", *J. Sound Vib.*, **187**(4), 695-712.

Wilson, E., Farhoomand, I. and Bathe, K. (1973), "Nonlinear dynamic analysis of complex structures", *Earthq. Eng. Struct. D.*, **1**(3), 241-252.

Wu, B., Wang, Qianying, W., Shing, B. and Ou, J. (2007), "Equivalent force control method for generalized real-time substructure testing with implicit integration", *Earthq. Eng. Struct. D.*, **36**(9), 1127-1149.

Wu, B., Wang, Z. and Bursi, O.S. (2012), "Nearly-perfect compensation for time delay in real-time hybrid simulation", *Proceedings of the 15WCEE, Lisboa*, Paper n.0507.

Nomenclature

A	Cross section area.
E	Young modulus.
EA	Axial stiffness.
g	Gravitational acceleration.
L	Effective length of the cable.
m	Mass per unit length.
T_s	Static tension of the cable.
T_d	Dynamic tension of the cable.
x, y, z	Cartesian global coordinates.
Γ	Ratio of cable weight to tension (= mgL/T).
$\in$	Static strain (=T/EA).
θ	Cable inclination angle.
λ^2	Irvine's non dimensional sag parameter (=$\Gamma^2 \cos^2 \theta/\in$).
ω_{yn}, ω_{zn}	Angular natural frequency of nth out-of-plane and in-plane modes respectively.
ω_g	Angular natural frequency of the deck.
ω_1	First out-of-plane angular natural frequency of the cable (=ω_{y1}).
ω_2	Second angular natural frequency of the cable.
q	Ratio of natural angular frequency of the deck to second natural angular frequency of the cable, ω_g/ω_2.